Chapter 1
Heat Transport in Low Dimensions: Introduction and Phenomenology

Stefano Lepri, Roberto Livi, and Antonio Politi

Abstract In this chapter we introduce some of the basic models and concepts that will be discussed throughout the volume. In particular we describe systems of nonlinear oscillators arranged on low-dimensional lattices and summarize the phenomenology of their transport properties.

1.1 Introduction

In this first chapter we review the main properties of low-dimensional lattices of coupled classical oscillators. We will describe how reduced dimensionality and conservation laws conspire in giving rise to unusual relaxation and transport properties. The aim is to provide both a general introduction to the general phenomenology and to guide the reader in the volume reading (where appropriate we indeed point to the more detailed analyses developed in the subsequent chapters).

For the sake of concreteness, one may think of quasi-1D objects, like long molecular chains or nanowires, suspended between two contacts which play the role of thermal reservoirs. These experimental setups, repeatedly discussed throughout the volume, are schematically depicted in Fig. 1.1.

We start Sect. 1.2 by introducing the main models without technicalities and providing the relevant definitions. Section 1.3 contains a summary of the different properties that is worth testing to characterize heat transport in a physical system.

S. Lepri (✉)
Consiglio Nazionale delle Ricerche, Istituto dei Sistemi Complessi, via Madonna del Piano 10, I-50019 Sesto Fiorentino, Italy
e-mail: stefano.lepri@isc.cnr.it

R. Livi
Dipartimento di Fisica e Astronomia and CSDC, Università di Firenze, via G. Sansone 1, I-50019 Sesto Fiorentino, Italy
e-mail: roberto.livi@unifi.it

A. Politi
Institute for Complex Systems and Mathematical Biology & SUPA University of Aberdeen, Aberdeen AB24 3UE, UK
e-mail: a.politi@abdn.ac.uk

S. Lepri (ed.), *Thermal Transport in Low Dimensions*, Lecture Notes in Physics 921, DOI 10.1007/978-3-319-29261-8_1

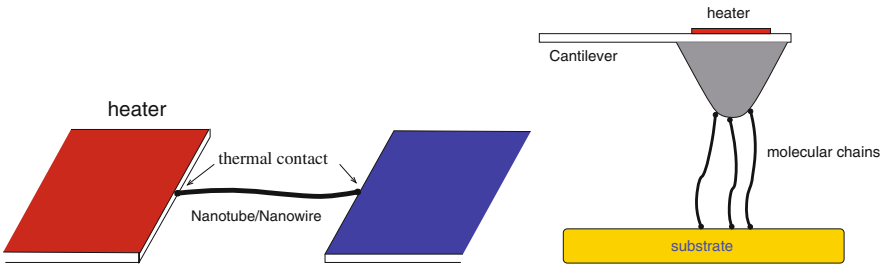

Fig. 1.1 Sketch of two experimental setups illustrating the physical setting. *Left*: a nanotube or nanowire suspended between two contacts acting as heaters and probes, see [14] and Chap. 8. *Right*: a scanning thermal microscopy setup whereby an assembly of molecular chains with one end attached on a substrate is heated through a cantilever tip [74]

The natural starting point is the effective conductivity in finite systems, which diverges with the system-size in the case of anomalous transport. The existence of long-time tails in the equilibrium correlation functions is another way of probing the system dynamics, together with the diffusion of localized perturbations and the relaxation of spontaneous fluctuations. Another, not much explored property, is the shape of the temperature profile that is strictly nonlinear even in the limit of small temperature differences, when heat transport is anomalous.

In Sect. 1.4, we present the overall scenario, making reference to the universality classes unveiled by the various theoretical approaches. More specifically, we emphasize the relationship with the evolution of rough interfaces and thereby the Kardar-Parisi-Zhang equation. Coupled rotors represent an important subclass of 1D systems where heat conduction is normal in spite of momentum conservation: their behavior is reviewed in Sect. 1.5.

The expected scenario in two-dimensions (namely the logarithmic divergence of heat conductivity) is discussed in Sect. 1.6, while the peculiar behavior of integrable systems is briefly reviewed in Sect. 1.7. In Sect. 1.8, we discuss the more general physical setup, where another quantity is being transported besides energy. This is the problem of coupled transport, where the interaction between the two processes may give rise to unexpected phenomena even when the transport is altogether normal. In particular, we consider a chain of coupled rotors in the presence of an additional torque, where the second quantity is angular momentum and the discrete nonlinear Schrödinger equation, where the second quantity is the norm (or mass). Finally, the still open problems are recalled in Sect. 1.9.

1.2 Models

The simplest microscopic dynamical model for the characterization of heat conduction consists of a chain of N classical point-like particles with mass m_n and position q_n, described by the Hamiltonian

$$H = \sum_{n=1}^{N} \left[\frac{p_n^2}{2m_n} + U(q_n) + V(q_{n+1} - q_n) \right] \quad . \tag{1.1}$$

The potential $V(x)$ accounts for the nearest-neighbour interactions between consecutive particles, while the on-site potential $U(q_n)$ takes into account the possible interaction with an external environment (either a substrate, or some three-dimensional matrix). The corresponding evolution equations are

$$m_n \ddot{q}_n = -U'(q_n) - F(r_n) + F(r_{n-1}) \quad , \quad n = 1, \ldots, N \, , \tag{1.2}$$

where $r_n = q_{n+1} - q_n$, $F(x) = -V'(x)$, and the prime denotes a derivative with respect to the argument. Usually q_n denotes the longitudinal position along the chain, so that

$$L = \sum_{n=1}^{N} r_n \, , \tag{1.3}$$

represents the total length of the chain (which, in the case of fixed b.c., is a constant of motion). Different kinds of boundary conditions may and will be indeed used in the various cases. For instance, if the particles are confined in a simulation "box" of length L with periodic boundary conditions,

$$q_{n+N} = q_n + L \quad . \tag{1.4}$$

Alternatively one can adopt a lattice interpretation, in which case, the (discrete) position is $z_n = an$ (where a is lattice spacing), while q_n is a transversal displacement. Thus, the chain length is obviously equal to Na.

The Hamiltonian (1.1) is generally a constant of motion. In the absence of an on-site potential ($U = 0$), the total momentum is conserved, as well,

$$P = \sum_{n=1}^{N} p_n \equiv \sum_{n=1}^{N} m_n \dot{q}_n \, . \tag{1.5}$$

Since we are interested in heat transport, one can set $P = 0$ (i.e., we assume to work in the center-of-mass reference frame) without loss of generality. As a result, the relevant state variables of microcanonical equilibrium are the specific energy (i.e., the energy per particle) $e = H/N$ and the elongation $\ell = L/N$ (i.e., the inverse of

the particle density). On a microscopic level, one can introduce three local densities, namely r_n, p_n and

$$e_n = \frac{p_n^2}{2m_n} + \frac{1}{2}\Big[V(r_n) + V(r_{n-1})\Big] \quad , \tag{1.6}$$

which, in turn, define a set of currents through three (discrete) continuity equations. For instance, the energy current is defined as

$$\dot{e}_n = j_{n-1} - j_n \tag{1.7}$$

$$j_n = \frac{1}{2} a(\dot{q}_{n+1} + \dot{q}_n)\, F(r_n) \quad . \tag{1.8}$$

The definition (1.8) is related to the general expression, originally derived by Irving and Kirkwood that is valid for every state of matter (see e.g. [53]) that, in one dimension, reads

$$j_n = \frac{1}{2}(q_{n+1} - q_n)(\dot{q}_{n+1} + \dot{q}_n)\, F(r_n) + \dot{q}_n e_n \,. \tag{1.9}$$

In the case of lattice systems, where we assume the limit of small oscillations (compared to the lattice spacing) or in the lattice field interpretation, one can recover formula (1.8) setting $q_{n+1} - q_n = a$ in the first term and neglecting the second one [64]. The expression (1.9) is useful in the opposite limit of freely colliding particles, where the only relevant interaction is the repulsive part of the potential, that is responsible for elastic collisions. There, the only contribution to the flux arises from the kinetic term of e_n, i.e.

$$j_n \approx \frac{1}{2} m_n \dot{q}_n^3 \quad . \tag{1.10}$$

Having set the basic definitions, let us now introduce some specific models. A first relevant example is the harmonic chain, where the potential V is quadratic (and $U = 0$). From the point of view of transport properties, we expect this system to behave like a ballistic conductor. The heat flux decomposes into the sum of independent contributions associated to the various eigenmodes. This notwithstanding, this model proves useful, as it allows addressing general questions about the nature of stationary nonequilibrium states. This includes the role of disorder (either in the masses or the spring constants), of boundary conditions, and quantum effects. Since the linear case (classical and quantum) will be treated in detail in Chap. 2, here we focus on the anharmonic problem. In this context, the most paradigmatic example is the Fermi–Pasta–Ulam (FPU) model [50, 76, 79]

$$V(r_n) = \frac{k_2}{2}(r_n - a)^2 + \frac{k_3}{3}(r_n - a)^3 + \frac{k_4}{4}(r_n - a)^4 \quad . \tag{1.11}$$

Following the notation of the original work [32], the couplings k_3 and k_4 are denoted by α and β respectively: historically this model is sometimes referred to as the "FPU-$\alpha\beta$" model. Also, the quadratic plus quartic ($k_3 = 0$) potential is termed the "FPU-β" model. Notice that upon introducing the displacement $u_n = q_n - na$ from the equilibrium position, r_n can be rewritten as $u_{n+1} - u_n + a$, so that the lattice spacing a disappears from the equations.

Another interesting model is the Hard Point Gas (HPG), where the interaction potential is [9, 40, 41]

$$V(y) = \begin{cases} \infty & \text{y} = 0 \\ 0 & \text{otherwise} \end{cases} .$$

The dynamics consist of successive collisions between neighbouring particles,

$$v_n' = \frac{m_n - m_{n+1}}{m_n + m_{n+1}} v_n + \frac{2m_{n+1}}{m_n + m_{n+1}} v_{n+1} \quad , \quad v_{n+1}' = \frac{2m_n}{m_n + m_{n+1}} v_n - \frac{m_n - m_{n+1}}{m_n + m_{n+1}} v_{n+1} \quad , \tag{1.12}$$

where m_n is the mass of the nth particle, $v_n = \dot{q}_n$ and the primed variables denote the values after the collision. For equal masses the model is completely integrable, as the set of initial velocities is conserved during the evolution. In order to avoid this peculiar situation, it is customary to choose alternating values, such as $m_n = m$ (rm) for even (odd) n. This type of dynamical systems are particularly appropriate for numerical computation as they do not require the numerical integration of nonlinear differential equations. In fact, it is sufficient to determine the successive collision times and update the velocities according to Eq. (1.12). The only errors are those due to machine round-off. Moreover, the simulation can be made very efficient by resorting to fast updating algorithms. In fact, since the collision times depend only on the position and velocities of neighbouring particles, they can be arranged in a heap structure and thereby simulate the dynamics with an event driven algorithm [40].

Another much studied model involves the Lennard–Jones potential, that in our units reads [66, 71]

$$V(y) = \frac{1}{12}\left(\frac{1}{y^{12}} - \frac{2}{y^6} + 1\right) . \tag{1.13}$$

For computational purposes, the coupling parameters have been fixed in such a way as to yield the simplest form for the force. With this choice, V has a minimum in $y = 1$ and the resulting dissociation energy is $V_0 = 1/12$. For the sake of convenience, the zero of the potential energy is set in $y = 1$. In one-dimension, the repulsive term ensures that the ordering is preserved (the particles do not cross each other).

In the presence of a substrate potential U, the invariance $q_l \to q_l + const.$ is broken and the total momentum P is no longer a constant of motion. Accordingly, all branches of the dispersion relation have a gap at zero wavenumber. We therefore

refer to them as *optical* modes. An important subclass is the one in which V is quadratic, which can be regarded as a discretization of the Klein-Gordon field: relevant examples are the Frenkel-Kontorova [39, 44] and "ϕ^4" models [1] which, in suitable units, correspond to $U(y) = 1 - \cos(y)$ and $U(y) = y^2/2 + y^4/4$, respectively. Another toy model that has been studied in some detail is the ding-a-ling system [11], where U is quadratic and the nearest-neighbor interactions are replaced by elastic collisions.

We will always deal with genuine nonintegrable dynamics. For the FPU model this means working with high enough energies/temperatures to avoid all the difficulties induced by quasi-integrability and the associated slow relaxation to equilibrium. For the diatomic HPG this requires fixing a mass-ratio r not too close to unity.

1.3 Signatures of Anomalous Transport

The results emerged from a long series of works can be summarized as follows. Models of the form (1.2) with $U(q) = 0$ typically display *anomalous* transport and relaxation features, this meaning that (at least) one of the following phenomena has been reported:

- The finite-size heat conductivity $\kappa(L)$ diverges in the limit of a large system size $L \to \infty$ [62] as[1]

$$\kappa(L) \propto L^{\alpha}$$

  This means that this transport coefficient is ill-defined in the thermodynamic limit;
- The equilibrium correlator of the energy current displays a nonintegrable power-law decay,

$$\langle J(t)J(0)\rangle \propto t^{-(1-\delta)} \tag{1.14}$$

  with $0 \leq \delta < 1$, for long times $t \to \infty$ [63]. Accordingly, the Green-Kubo formula yields an infinite value of the conductivity;
- Energy perturbations propagate superdiffusively [15, 24]: a local perturbation of the energy broadens and its variance σ^2 grows in time as

$$\sigma^2(t) \propto t^{\beta} \tag{1.15}$$

  with $\beta > 1$;

[1] For historical reasons two of the scaling exponents introduced in this section are conventionally denoted by the same Greek letters, α and β, adopted for the FPU models described in Sect. 1.2.

- Relaxation of spontaneous fluctuations is fast (i.e. superexponential) [66]: at variance with standard hydrodynamics, the typical decay rate in time of fluctuations at wavenumber k, $\tau(k)$, is found to scale as

$$\tau(k) \sim |k|^{-z}$$

(with $z < 2$).
- Temperature profiles in the nonequilibrium steady states are nonlinear, even for vanishing applied temperature gradients.

Altogether, these features can be summarized by saying that the usual Fourier's law *does not hold*: the kinetics of energy carriers is so correlated that they are able to propagate *faster* than in the the standard (diffusive) case.

Numerical studies [64] indicate that anomalies occur generically in 1 and 2D, whenever the conservation of energy, momentum and length holds. This is related to the existence of long-wavelength (Goldstone) modes (an acoustic phonon branch in the linear spectrum of (1.2) with $U = 0$) that are very weakly damped. Indeed, it is sufficient to add external (e.g. substrate) forces, to make the anomalies disappear.

Let us now discuss these features in more detail.

1.3.1 Diverging Finite-Size Conductivity

A natural way to simulate a heat conduction experiment consists in putting the system in contact with two heat reservoirs operating at different temperatures T_+ and T_- (see Fig. 1.2). This requires a suitable modeling of interaction with the environment. Several methods, based on both deterministic and stochastic algorithms, have been proposed. A more detailed presentation can be found in [26, 64]. A simple and widely used choice consists in adding Langevin-type forces on some chain subsets. If this is done on the first and the last site of a finite chain ($n = 1, \ldots, N$), it is obtained

$$\ddot{q}_n = -F_n + F_{n-1} + \delta_{n1}(\xi_+ - \lambda \dot{q}_1) + \delta_{nN}(\xi_- - \lambda \dot{q}_N) \quad , \tag{1.16}$$

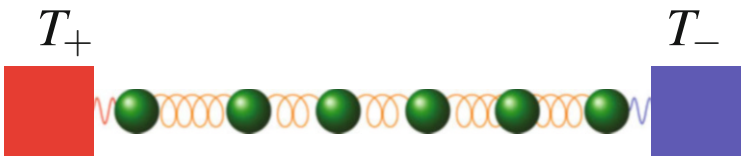

Fig. 1.2 A one-dimensional chain of coupled oscillators interacting with two thermal reservoirs ad different temperatures T_+ and T_-

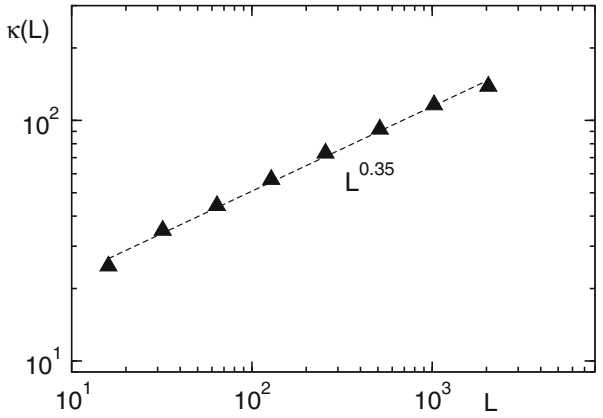

Fig. 1.3 Scaling of the finite-size conductivity for the FPU-$\alpha\beta$ model: with energy $e = 1$ and cubic coupling constant $\alpha = 0.1$

where we assume unitary-mass particles, while $\xi_\pm$'s are two independent Gaussian processes with zero mean and variance $2\lambda k_B T_\pm$ (k_B is the Boltzmann constant). The coefficient λ is the coupling strength with the heat baths.

After a long enough transient, an off-equilibrium stationary state sets in, with a net heat current flowing through the lattice.[2] The thermal conductivity κ of the chain is then estimated as the ratio between the time-averaged flux $\bar{j}$ and the overall temperature gradient $(T_+ - T_-)/L$, where L is the chain length. Notice that, by this latter choice, κ amounts to an effective transport coefficient, including both boundary and bulk scattering mechanisms. The average $\bar{j}$ can be estimated in several equivalent ways, depending on the employed thermostatting scheme. One possibility is to directly measure the energy exchanges with the two heat reservoirs [26, 64]. A more general (thermostat-independent) definition consists in averaging the heat flux as defined by (1.9).

As a result of many independent simulations performed with the above-described methods, it is now established that $\kappa \propto L^\alpha$ for L large enough. Figure 1.3 illustrates the typical outcome of simulations for the FPU chain.

1.3.2 Long-Time Tails

In the spirit of linear-response theory, transport coefficients can be computed from equilibrium fluctuations of the associated currents. More precisely, by introducing

[2]From the mathematical point of view, the existence of a unique stationary measure is a relevant question and has been proven in some specific cases models of this class, see the review [8, 28, 29].

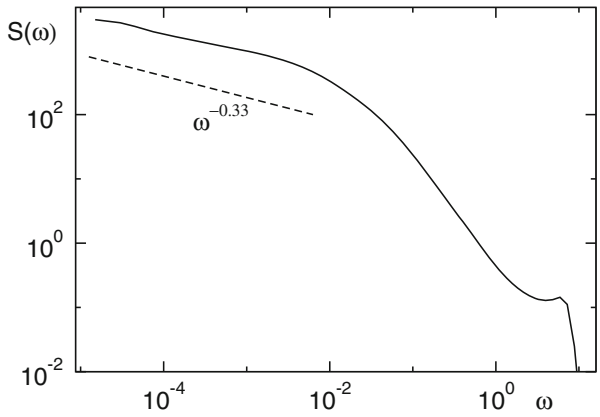

Fig. 1.4 Spectrum of energy current for the FPU-$\alpha\beta$ model, same parameters as in previous figure

the total heat flux

$$J = \sum_n j_n \quad , \tag{1.17}$$

the Green-Kubo formalism tells us that heat conductivity is given by the expression

$$\kappa \;=\; \frac{1}{k_B T^2} \lim_{t\to\infty} \lim_{N\to\infty} \frac{1}{N} \int_0^t dt' \, \langle J(t')J(0)\rangle \quad , \tag{1.18}$$

where the average is performed in a suitable equilibrium ensemble, e.g. microcanonical with zero total momentum ($P = 0$).

A condition for the formula (1.18) to give a well-defined heat conductivity is that the time integral is convergent. This is clearly not the case when the current correlator vanishes as in (1.14) with $0 \leq \delta < 1$. Here, the integral diverges as t^δ and we may thus define a finite-size conductivity $\kappa(L)$ by truncating the time integral in the above equation to $t \approx L/c$, where c is the sound velocity. Consistency with the definition of the power-law divergence of $\kappa(L)$ implies $\alpha = \delta$. The available data agrees with this expectation, thus providing an independent method for estimating the exponent α.

For later purposes, we mention that, by means of the Wiener–Khintchine theorem, one can equivalently extract δ from the low-frequency behavior of the spectrum of current fluctuations

$$S(\omega) \equiv \int d\omega \langle J(t)J(0)\rangle \mathrm{e}^{i\omega t} \tag{1.19}$$

that displays a low-frequency singularity of the form $S(\omega) \propto \omega^{-\delta}$ (see Fig. 1.4). From the practical point of view, this turns out to be the most accurate numerical strategy, as divergencies are better estimated than convergences to zero.

1.3.3 Diffusion of Perturbations

Consider an infinite system at equilibrium with a specific energy e_0 per particle and a total momentum $P = 0$. Let us perturb it by increasing the energy of a subset of adjacent particles by some preassigned amount Δe and denote with $e(x,t)$ the energy profile evolving from such a perturbed initial condition (for simplicity, we identify x with the average particle location $n\ell$). We then ask how the perturbation

$$\delta e(x,t) = \langle e(x,t) - e_0 \rangle \tag{1.20}$$

behaves in time and space [42], where the angular brackets denote an ensemble average over independent trajectories. Because of energy conservation, $\sum_n \delta e(n\ell, t) = \Delta e$ remains constant at any time: $\delta e(x,t)$ can be interpreted as a probability density (provided it is also positive-defined and normalized).

For sufficiently long time t and large x, one expects $\delta e(x,t)$ to scale as

$$\delta e(x,t) = t^{-\gamma} \mathscr{G}(x/t^{\gamma}) \tag{1.21}$$

for some probability distribution $\mathscr{G}$ and a scaling parameter $0 \leq \gamma \leq 1$. The case $\gamma = 1/2$ corresponds to a normal diffusion and to a normal conductivity. On the other hand, $\gamma = 1$ corresponds to a ballistic motion and to a linear divergence of the conductivity. Consequently, a γ-value larger than $1/2$ implies a superdiffusive behavior of the macroscopic evolution of the energy perturbation [24]. In Fig. 1.5, the evolution of infinitesimal energy perturbations is reported in the case of the HPG [15]: a very good data-collapse is reported for $\gamma = 3/5$.

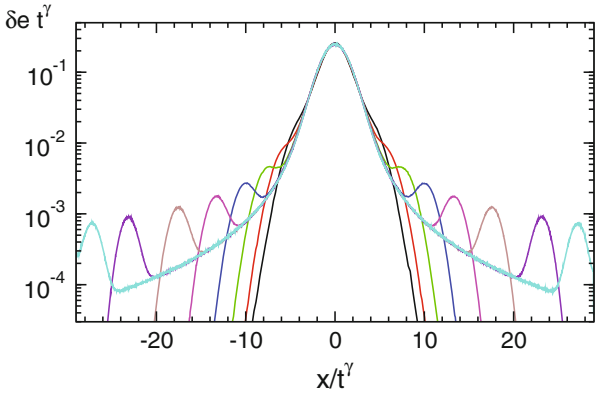

Fig. 1.5 Spreading of infinitesimal perturbations in the HPG model: rescaled perturbation profiles at different times $t = 40, 80, 160, 320, 640, 1280, 2560, 3840$ (the width increases with time), with $\gamma = 3/5$

Remarkably, the above results can be rationalized in terms of a very simple random dynamics: the *Lévy walk model* [7, 95]. Consider a point particle that moves ballistically in between successive "collisions", whose time separation is distributed according to a power law, $\psi(t) \propto t^{-\mu-1}$, $\mu > 0$, while its velocity is chosen from a symmetric distribution $\Psi(v)$. By assuming a δ-like distribution, $\Psi(v) = (\delta(v-\tilde{v}) + \delta(v+\tilde{v}))/2$, the propagator $P(x,t)$ (the probability distribution function to find in x at time t, a particle initially localized at $x = 0$) can be written as $P(x,t) = P_L(x,t) + t^{1-\mu}[\delta(x-\tilde{v}t) + \delta(x-\tilde{v}t)]$ where [7]

$$P_L(x,t) \propto \begin{cases} t^{-1/\mu} \exp\left[-(\eta x/t^{1/\mu})^2\right] & |x| < t^{1/\mu} \\ t\,x^{-\mu-1} & t^{1/\mu}, |x| < \tilde{v}t \\ 0 & |x| > \tilde{v}t \end{cases} , \tag{1.22}$$

where η is a generalized diffusion coefficient. From the evolution of the perturbation profile, it is possible to infer the exponent α of the thermal conductivity. In fact, in [24] it has been argued that the exponents α, β (the growth rate of the mean square displacement, $\sigma^2(t) = \sum_n n^2 \delta e(x = n\ell, t) \propto t^\beta$) and $\gamma = 1/\mu$ are linked by the following relationships,

$$\alpha = \beta - 1 = 2 - \frac{1}{\gamma}. \tag{1.23}$$

In particular, we see that the case $\gamma = 1/2$ corresponds to normal diffusion ($\beta = 1$) and to a normal conductivity ($\alpha = 0$). On the other hand, $\gamma = 1$ corresponds to a ballistic motion ($\beta = 2$) and to a linear divergence of the conductivity ($\alpha = 1$). The numerically observed value $\gamma = 3/5$ corresponds to an anomalous divergence with $\alpha = 1/3$.

The spreading of the wings can be accounted by means of a model which allows for velocity fluctuations [25, 94], which originates from wave dispersion. Assigning smoother velocity distributions $\Psi(v)$ leads to broadening of δ side-peaks, but does not affect the shape and the scaling behavior of the bulk contribution $P_L(x,t)$, which scales, as predicted in Eq. (1.21), with the exponent $\gamma = 1/\mu$.

An alternative way to study finite amplitude perturbations is by looking directly at the behavior of the nonequilibrium correlation function of the energy density [96],

$$C_e(x,t) = \langle \delta e(y,\tau) \delta e(x+y, t+\tau) \rangle \quad , \tag{1.24}$$

where the angular brackets denote a spatial as well as a temporal average over the variables y and τ, respectively. At $t = 0$, $C_e(x,0)$ is a δ function in space. Moreover, in the microcanonical ensemble, energy conservation implies that the area $\int dx C_e(x,t)$ is constant at any time. By assuming that $C_e(x,t)$ is normalized to a unit area, its behavior is formally equivalent to that of a diffusing probability distribution. This allows one to determine the scaling behavior of the heat conductivity from the growth rate of the variance of $C_e(x,t)$ [96]. As the determination of the variance is troubled by the fluctuating tails, it is preferable to proceed by looking at the decay

of the maximum $C_e(0,t)$, that is statistically more reliable. An interesting relation between correlation function and anomalous heat transport has been pointed out recently [69] and is reviewed in Chap. 6.

1.3.4 Relaxation of Spontaneous Fluctuations

The above discussion suggests that scaling concepts can be of great importance in dealing with thermal fluctuations of conserved quantities. The evolution of a fluctuation of wavenumber k excited at $t = 0$ is described by its correlation function. For 1D models like (1.1) one of such functions is defined by considering the relative displacements $u_n = q_n - n\ell$ and defining the collective coordinates through the discrete transform

$$U(k,t) = \frac{1}{N}\sum_{n=1}^{N} u_n \exp(-ikn) \quad . \tag{1.25}$$

By virtue of the periodic boundaries, the allowed values of the wavenumbers k are integer multiples of $2\pi/N$. We then define the dynamical structure factor, namely the square modulus of the temporal Fourier transform of the particle displacements as

$$S(k,\omega) = \left\langle \left| U(k,\omega) \right|^2 \right\rangle \quad . \tag{1.26}$$

The angular brackets denote an average over an equilibrium ensemble.

For sufficiently small wavenumbers k, the dynamical structure factor $S(k,\omega)$ usually displays sharp peaks at finite frequency, whose position is proportional to the wavenumber $\omega_{max} = c|k|$; c is naturally interpreted as the phonon sound speed. The data in Fig. 1.6 show that long-wavelength correlations, $k \to 0$, obey *dynamical*

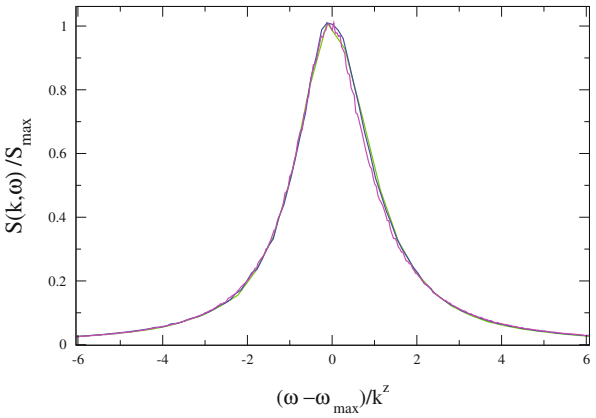

Fig. 1.6 FPU$\alpha\beta$ model: check of dynamical scaling for the dynamical structure factors $\alpha = 0.1$, $N = 4096$, $e = 0.5$ and four different wavenumbers $k = 2, 4, 8, 16$ (in units of $2\pi/N$). The best estimate of the dynamical exponent is $z = 1.5$

scaling, i.e. there exist a function f such that

$$S(k,\omega) \sim f\left(\frac{\omega - \omega_{max}}{k^z}\right). \tag{1.27}$$

for ω close enough to ω_{max}. The associated linewidths are a measure of the fluctuation's inverse lifetime. Simulations indicate that these lifetimes scale as k^{-z} with $z \approx 1.5$. Thus the behavior is different from the diffusive one where one would expect $z = 2$. As explained above, one may think of this as a further signature of an underlying superdiffusive process, intermediate between standard Brownian motion and ballistic propagation.

Other correlation functions can be defined similarly and obey some form of dynamical scaling. For instance, one could consider the structure factor $S_e(k,\omega)$ associated with the local energy density e_n, defined in (1.6). It has a large central component (as a result of the heat modes) and a ballistic one (following from the sound modes). If we assume that the low-frequency part is dominated by the heat-mode scaling, we should have for $\omega \to 0$

$$S_e(k,\omega) \sim g(\omega/q^{5/3}) \,, \tag{1.28}$$

with g being a suitable scaling function.

The origin of the nontrivial dynamical exponents is to be traced back to the nonlinear interaction of long-wavelength fluctuations. For a chain of coupled anharmonic oscillators with three conserved fields (H, L, and P), a linear theory would yield two propagating sound modes and one diffusing heat mode, all of the three diffusively broadened. In contrast, the nonlinear theory predicts that, at long times, the sound mode correlations satisfy Kardar-Parisi-Zhang scaling, while the heat mode correlations follow a Lévy-walk scaling. Various spatiotemporal correlation functions of Fermi-Pasta-Ulam chains and a comparison with the theoretical predictions can be found in [17].

1.3.5 Temperature Profiles

Anomalous transport manifests itself also in the shape of the steady-state temperature profiles. For chains in contact with two baths like in Eq. (1.16), one typically observes that the kinetic temperature profile $T_n = \langle p_n^2 \rangle$ is distinctly nonlinear also for small temperature differences ΔT. For fixed ΔT, the profile typically satisfies a "macroscopic" scaling, $T_n = T(n/L)$ for $L \to \infty$ with $T(0) = T_+$ and $T(1) = T_-$.[3]

[3]Temperature discontinuities may appear at the chain boundaries. This is a manifestation of the well-known Kapitza resistance, the temperature discontinuity arising when a heat flux is maintained across an interface among two substances. This discontinuity is the result of a boundary

In view of the above correspondence with Lèvy processes it may be argued that this feature too could be described in terms of anomalous diffusing particles in a finite domain and subject to external sources that steadily inject particles through its boundaries. The idea is to interpret the local temperature $T(x)$ as the density $P(x)$ of suitable random walkers. A general stochastic model can be defined as follows [61]. Let n denote the position of a discrete-time random walker on a finite one-dimensional lattice ($1 \leq n \leq N$). In between consecutive scattering events, the particle either jumps instantaneously (Lévy flight—LF) or moves with unit velocity (Lévy walk—LW) over a distance of m sites, that is randomly selected according to the step-length distribution

$$\lambda_m = \frac{q}{|m|^{1+\mu}}, \quad \lambda_0 = 0 \,, \tag{1.29}$$

which is the discrete analogous of the ψ distribution defined above, with μ ($1 \leq \mu \leq 2$) being the Lévy exponent and q a normalization constant. The process can be formulated by introducing the vector $\mathbf{W} \equiv \{W_n(t)\}$, where W_n is the probability for the walker to undergo a scattering event at site n and time t. It satisfies a master equation, which, for LFs, writes

$$\mathbf{W}(t+1) = \mathbf{Q}\mathbf{W}(t) + \mathbf{S}, \tag{1.30}$$

where $\mathbf{S}$ accounts for the particles steadily injected from external reservoirs; $\mathbf{Q}$ is a matrix describing the probability of paths connecting pair of sites. In the simple case of absorbing BC, it is readily seen that Q_{ji} is equal to the probability λ_{j-i} of a direct flight, as from Eq. (1.29). In the LW case, the $\mathbf{W}$ components in the r.h.s. must be estimated at different times (depending on the length of the path followed from j to i) [52]. Since, the stationary solution is the same in both cases, this difference is immaterial, and is easier to refer to LFs, since Eq. (1.30) can be solved iteratively. Note that in the LF case, W_i is equal to the density P_i of particles at site i, while for the LW, P_i includes those particles that are transiting at the ith site during a ballistic step.

The source term is fixed by assuming that the reservoir is a semi-infinite lattice, homogeneously filled by Lévy walkers of the same type as those residing in the domain. This amounts to defining $S_m = s\, m^{-\mu}$, where s measures the density of particles and m the distance from the reservoir. It is easy to verify that in the presence of two identical reservoirs at the lattice ends, the density is constant (for any N), showing that our definition satisfies a kind of "zeroth principle", as it should.

In the nonequilibrium case, it is not necessary to deal with two reservoirs. The linearity of the problem teaches us that it is sufficient to study the case of a single reservoir, that we assume to be in $n = 0$: the effect of, say, a second one on the

resistance, that is explained as a "phonon mismatch" between the two media: see [2] for a discussion of the class of models at hand.

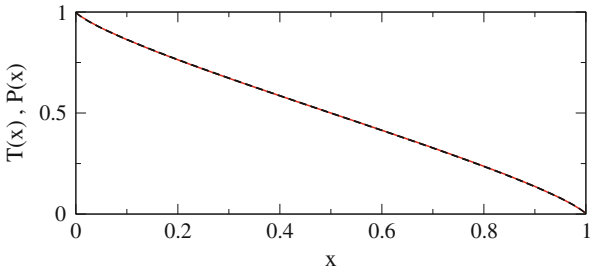

Fig. 1.7 Temperature profile $T(x)$ of the oscillator chain with conservative noise with free boundary condition and $\lambda = \gamma = 1$ (*solid line*) and density profile $P(x)$ for the master equation with reflection coefficient $r = -0.1$ (*dashed line*)

opposite side can be accounted for by a suitable linear combination. For large-enough N values, the steady-state density depends on n and N through the combined variable $x = n/N$, i.e. $P(x) = P_n$. As seen in Fig. 1.7, P vanishes for $x \to 1$ because on that side the absorbing boundary is not accompanied by an incoming flux of particles.

Altogether, upon identifying the particle density with the temperature, the profile can be viewed as a stationary solution of the stationary Fractional Diffusion Equation (FDE)

$$D_x^{\mu} P = -\sigma(x) \tag{1.31}$$

on the interval $0 \leq x \leq 1$ (see e.g. [98] and references therein for the definition of the integral operator D_x^{μ}). The source term $\sigma(x)$ must be chosen so as to describe the effect of the external reservoirs. A condition to be fulfilled is that two identical reservoirs yield a homogeneous state $T(x) = const$. Using the integral definition of D_x^{μ} [98], it can be shown that this happens for $\sigma(x) = \sigma_{eq}(x) \equiv x^{-\mu} + (1-x)^{-\mu}$ (we, henceforth, ignore irrelevant proportionality constants). It is thus natural to associate $\sigma(x) = x^{-\mu}$ to the nonequilibrium case with a single source in $x = 0$. The numerical solution of the FDE agrees perfectly with the stationary solution of the discrete model, thus showing that long-ranged sources are needed to reproduce the profiles in the continuum limit.

A distinctive feature of the profile is that it is not analytic at the boundaries. Indeed, the data for $x \to 0$ are well fitted by

$$P(x) \;=\; P(0) + Cx^{\mu_m} \tag{1.32}$$

(the same behavior occurs for $x \to 1$, as the profiles are symmetric). In view of the similarity with the shape of the liquid surface close to a wall, we metaphorically term μ_m as the *meniscus exponent*. Such nonanalytic behavior is peculiar of anomalous kinetics, as opposed to the familiar linear shape in standard diffusion. For the above discussed case of absorbing BC, we find that $\mu_m \approx \mu/2$. This value is consistent

with the singular behavior of the eigenfunctions of D_x^{μ} [98]. In the general case, by assuming a linear dependence of μ_m on both r, and μ, it has been conjectured that [61]

$$\mu_m = \frac{\mu}{2} + r\left(\frac{\mu}{2} - 1\right) . \tag{1.33}$$

This expression is consistent with the $\mu_m = \alpha/2$ value found above for $r = 0$. Moreover, for $\alpha = 2$ (normal diffusion) it yields $\mu_m = 1$, as it should.

Let us now compare this probability distribution of the above process with the temperature profiles in one-dimensional systems displaying anomalous energy transport. It is convenient to refer to a chain of harmonic oscillators coupled with two Langevin heat baths (with a damping constant λ), and with random collisions that exchange the velocities of neighboring particles with a rate γ [23]. On the one hand, this model has the advantage of allowing for an exact solution of the associated Fokker-Planck equation [67]; on the other hand it is closely related to a model that has been proved to display a Lévy-type dynamics [4].

In Fig. 1.7 we compare the temperature profile $T(x)$ (suitably shifted and rescaled) of the heat-conduction model [67] with free BC and the solution of our discrete Lévy model with a reflection coefficient $r = -0.1$. Since they are essentially indistinguishable, we can conclude that the Lévy interpretation does not only allow explaining the anomalous scaling of heat conductivity [15], but also the peculiar shape of $T(x)$. The weird (negative) value of r can be justified a posteriori by introducing two families of walkers and interpreting the reflection as a change of family. The relevant quantity to look at is the difference between the densities of the two different families. The reason why it is necessary to invoke the presence of such two families and their physical meaning in the context of heat conductivity is an open problem.

In the case of a chain with fixed BC, the temperature profile $T(x)$ can be computed analytically [67] and it is thereby found that $\mu_m = 1/2$. By inserting this value in Eq. (1.33) and recalling that $\mu = 3/2$, we find that $r = 1$, i.e. the fixed-BC $T(x)$ corresponds to the case of perfectly reflecting barriers. Unfortunately, this (physically reasonable) result could not be tested quantitatively. Indeed, it turns out that finite-size corrections become increasingly important upon increasing r, and for r close to 1, it is practically impossible to achieve convergence to the steady-state.

The description of the steady state in terms of Lévy walk has been further investigated in [27]. The authors calculate exactly the average heat current, the large deviation function of its fluctuations, and the temperature profile in the steady state. The current is nonlocally connected to the temperature gradient. Also, all the cumulants of the current fluctuations have the same system-size dependence in the open geometry as those of deterministic models like the HPG. The authors investigated also the case of a ring geometry and argued that a size-dependent cutoff time is necessary for the Lévy-walk model to behave like in the deterministic case. This modification does not affect the results on transport in the open geometry for large enough system sizes.

1.4 Universality and Theoretical Approaches

In view of their common physical origin, it is expected that the exponents describing the different processes will be related to each other by some "hyperscaling relations". Their value should be ultimately dictated by the dynamical scaling of the underlying dynamics. Moreover, one can hope that they are largely independent of the microscopic details, thus allowing for a classification of anomalous behavior in terms of "universality classes". This crucial question is connected to the predictive power of simplified models and to the possibility of applying theoretical results to real low-dimensional materials.

1.4.1 Methods

Various theoretical approaches to account for the observed phenomenology have been developed and implemented. In the rest of the volume they will be exposed in detail; here we limit ourselves to a brief description. The methods discussed are

1. *Fluctuating hydrodynamics* approach: here the models are described in terms of the random fields of deviations of the conserved quantities with respect to their stationary values. The role of fluctuations is taken into account by renormalization group or some kind of self-consistent theory.
2. *Mode-coupling* theory: this is closely related to the above, as it amounts to solving (self-consistently) some approximate equations for the correlation functions of the fluctuating random fields.
3. *Kinetic theory*: it is based on the familiar approach to phonon transport by means of the Boltzmann equation.
4. *Exact solution* of specific models: typically in this case the original microscopic Hamiltonian dynamics is replaced by some suitable stochastic one which can be treated by probabilistic methods.

A sound theoretical basis for the idea that the above described anomalies are generic and universal for all momentum-conserving system was put forward in [77]. The authors treated the case of a fluctuating d-dimensional fluid and applied renormalization group techniques to evaluate the contribution of noisy terms to transport coefficients. The calculation predicts that the thermal conductivity exponent is $\alpha = (2-d)/(2+d)$. From the arguments exposed above, it follows that in 1D the exponents are

$$\alpha = \delta = \frac{1}{3}, \qquad \beta = \frac{4}{3}, \qquad z = \frac{3}{2} \quad . \tag{1.34}$$

According to this approach, any possible additional term in the noisy Navier-Stokes equation yields irrelevant corrections in the renormalization procedure, meaning

that the above exponents are model independent, provided the basic conservation laws are respected.

Next we give a flavour of one of the other approaches: the Mode-Coupling Theory (MCT). This type of theories has been traditionally invoked to estimate long-time tails of fluids [82] and to describe the glass transition [87]. In the simplest version, it involves the normalized correlator of the particle displacement [see Eq.(1.25)], where the discrete wavenumber k has been turned to the continuous variable q)

$$G(q,t) = \frac{\langle U^*(q,t)U(q,0)\rangle}{\langle |U(q)|^2\rangle} \ .$$

$G(q,t)$ is akin to the density–density correlator, an observable routinely used in condensed-matter physics. The main idea is to write a set of approximate equations for $G(q,t)$ that must be solved self-consistently. For the problem at hand, the simplest version of the theory amounts to consider the equations [60, 86]

$$\ddot{G}(q,t) + \varepsilon \int_0^t \Gamma(q,t-s)\dot{G}(q,s)\,ds + \omega^2(q)G(q,t) = 0 \quad , \tag{1.35}$$

where the memory kernel $\Gamma(q,t)$ is proportional to $\langle \mathscr{F}(q,t)\mathscr{F}(q,0)\rangle$, with $\mathscr{F}(q)$ being the nonlinear part of the fluctuating force between particles. Equation (1.35) is derived within the well-known Mori–Zwanzig projection approach [53]. It must be solved with the initial conditions $G(q,0) = 1$ and $\dot{G}(q,0) = 0$.

The mode-coupling approach basically amounts to replacing the exact memory function Γ with an approximate one, where higher-orders correlators are written in terms of $G(q,t)$. In the generic case, in which k_3 is different from zero [see Eq. (1.11)], the lowest-order mode coupling approximation of the memory kernel turns out to be [60, 86]

$$\Gamma(q,t) = \omega^2(q)\,\frac{2\pi}{N} \sum_{p+p'-q=0,\pm\pi} G(p,t)G(p',t) \quad . \tag{1.36}$$

Here p and p' range over the whole Brillouin zone (from $-\pi$ to π in our units) . This yields a closed system of nonlinear integro-differential equations. Both the coupling constant ε and the frequency $\omega(q)$ are temperature-dependent input parameters, which should be computed independently by numerical simulations or approximate analytical estimates. For the present purposes it is sufficient to restrict ourselves to considering their bare values, obtained in the harmonic approximation. In the adopted dimensionless units they read $\varepsilon = 3k_3^2 k_B T/2\pi$ and $\omega(q) = 2|\sin\frac{q}{2}|$. Of course, the actual renormalized values are needed for a quantitative comparison with specific models. The long-time behavior of G can be determined by looking for a solution of the form

$$G(q,t) \ = \ C(q,t)e^{i\omega(q)t} + c.c. \tag{1.37}$$

with $\dot{G} \ll \omega G$. It can thus be shown [19, 21] that, for small q-values and long times $C(q,t) = g(\sqrt{\varepsilon}tq^{3/2})$ i.e. $z = 3/2$ in agreement with the above mentioned numerics. Furthermore, in the limit $\sqrt{\varepsilon}tq^{3/2} \to 0$ one can explicitly evaluate the functional form of g, obtaining

$$C(q,t) = \frac{1}{2}\exp\left(-Dq^2|t|^{\frac{4}{3}}\right) \quad , \tag{1.38}$$

where D is a suitable constant of order unity. The correlation displays a "compressed exponential" behavior in this time range. This also means that the lineshapes of the structure factors $S(q,\omega)$ are non-Lorentzian but rather exhibit an unusual faster power-law decay $(\omega - \omega_{max})^{-7/3}$ around their maximum. Upon inserting this scaling result into the definition of the heat flux, one eventually concludes that the conductivity exponent is $\alpha = 1/3$, in agreement with (1.34).

A more refined theory requires considering the mutual interaction among *all* the hydrodynamic modes associated with the conservation laws of the system at hand. The resulting calculations are considerably more complicated but they can be worked out [88, 89]. As a result, the same values of the scaling exponents are found, but also a more comprehensive understanding is achieved (see Chap. 3 for a detailed account).

1.4.2 Connection with the Interface Problem

Relevant theoretical insight comes from the link with one of the most important equations in nonequilibrium statistical physics, the Kardar-Parisi-Zhang (KPZ) equation. This is a nonlinear stochastic Langevin equation which was originally introduced in the (seemingly unrelated) context of surface growth [3]. Let us first consider the fluctuating Burgers equation for the random field $\rho(x,t)$

$$\frac{\partial\rho}{\partial t} = \frac{\lambda}{2}\frac{\partial\rho^2}{\partial x} + D\frac{\partial^2\rho}{\partial x^2} + \frac{\partial\eta}{\partial x}, \tag{1.39}$$

where $\eta(x,t)$ represents a Gaussian white noise with $\langle\eta(x,t)\eta(x',t')\rangle = 2D\delta(x-x')\delta(t-t')$. As it is well-known, Eq. (1.39) can be transformed into the KPZ equation by introducing the "height function" h such that $\rho = \frac{\partial h}{\partial x}$,

$$\frac{\partial h}{\partial t} = \frac{\lambda}{2}\left(\frac{\partial h}{\partial x}\right)^2 + D\frac{\partial^2 h}{\partial x^2} + \eta. \tag{1.40}$$

It has been shown [89] that the mode-coupling approximation for the correlator of ρ obeying (1.39) is basically identical to the equation for C described in the previous paragraph. Thus one may argue that the dynamical properties are those of the KPZ equation in one dimension. Loosely speaking, we can represent the displacement

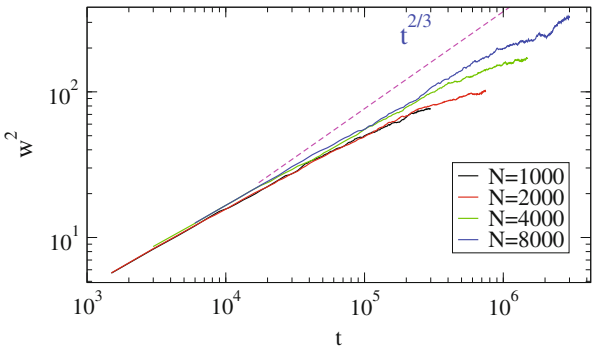

Fig. 1.8 Evolution of the variance (1.41) for the FPU $\alpha\beta$ chain with $e = 0.5$ $\alpha = 0.1$ and for increasing chain lengths N (bottom to top solid lines). The *dashed line* is the expected KPZ growth rate

field as the superposition of counterpropagating plane waves modulated by an envelope that is ruled, at large scales, by Eq. (1.40).

In order to illustrate this, we have performed a typical "KPZ numerical experiment" [3] for the for the FPU $\alpha\beta$ chain. In practice, we monitored

$$w^2(t,N) = \left\langle \frac{1}{N}\sum_n h_n^2 - (\frac{1}{N}\sum_n h_n)^2 \right\rangle \tag{1.41}$$

where $h_n(t) = q_n(t) - q_n(0)$, $q_n(0)$ is an equilibrium configuration and the angular brackets denote an average over an ensemble of different trajectories. The results are reported in Fig. 1.8. The only difference with respect to the usual setup is that here the square-width is plotted only at times t multiples of L/c, where c is the effective sound speed. These are the only moments, when the effect of counterpropagating sound waves cancel out, offering the chance to identify a KPZ-like behavior. In fact, one can see that the growth in Fig. 1.8 is compatible with the expected KPZ exponent 2/3 (actually, a bit smaller) followed by a saturation due to the finite size of the chain. A more rigorous discussion of the above topics can be found in Chap. 3.

1.4.3 Other Universality Classes

In the previous section we argued that the scaling properties of anomalous transport are independent of the microscopic details and correspond to those of the KPZ universality class. One might wonder whether other classes exist and under which conditions they can be observed. A reasonable argument, that can be invoked to delimit the KPZ universality class, is the *symmetry* of the interaction potential with respect to the equilibrium position. With reference to the MCT, one realizes that the symmetry of the fluctuations implies that the quadratic kernel in (1.36) should be

replaced by a cubic one,[4] thus yielding different values of the exponents [21]. In the language of KPZ interfaces, whenever the coefficient of the nonlinear term vanishes, the evolution equation reduces to the Edwards-Wilkinson equation that is indeed characterized by different scaling exponents. The argument can be made more precise in the framework of the full hydrodynamic theory [88, 89]. There, different dynamical exponents can arise if the coupling between some modes vanishes (we refer again the reader to Chap. 3 for a detailed discussion). A thermodynamic interpretation of this difference is given in [57, 58].

The FPU model is a natural instance to test this working hypothesis. In fact, systematically larger values of the scaling exponent α have been reported for the FPU-β case where the cubic term of the potential is absent [65]. The existence of two universality classes for thermal transport in one-dimensional oscillator systems has been also demonstrated in [55], where it was further proposed that the criterion for being out of the KPZ class is the condition $\gamma = c_P/c_V = 1$, where c_P and c_V are the specific heat capacities at constant pressure and volume, respectively.

The scenario can be further illustrated by considering a modification of the HPG model, the so-called Hard-Point Chain (HPC) [20], characterized by a square-well potential in the relative distances

$$V(y) = \begin{cases} 0 & 0 < \mathrm{y} < \mathrm{a} \\ \infty & \text{otherwise} \end{cases} . \tag{1.42}$$

The infinite barriers at $y = a$ imply an elastic "rebounding" of particles as if they were linked by an inextensible and massless string of fixed length a. The string has no effect on the motion, unless it reaches its maximal length, when it exerts a restoring force that tends to rebound the particles one against the other. The potential (1.42) introduces the physical distance a as a parameter of the model.

As it is well known, the thermodynamics of models like the HPC can be solved exactly and the equation of state is found to be

$$L = N\left[\frac{1}{\beta P} - \frac{a}{\exp(\beta P a) - 1}\right]$$

where P is the pressure of the HPC. Note that, for large values of a, the equation of state is the same of an HPC i.e. the one of an ideal gas in 1D. The important point here is that we can choose the parameter a such as $P = 0$. In this particular point the interaction is symmetric ($L/N = a/2$).

A peculiarity of the HPC model is that energy transfer occurs also at rebounding "collisions" at distance a, this means that besides the contribution defined by Eq. (1.10) one should include a term j_i' as from Eq. (1.9). However, one cannot

[4] In fact, the quadratic kernel corresponds to a quadratic force originating from the leading cubic nonlinearity of any asymmetric interaction potential, while a quartic leading nonlinearity of a symmetric interaction potential yields a cubic kernel (force).

proceed directly, since the force is singular, there. By defining the force between two particles as the momentum difference induced by a collision, j_i' can be written as the kinetic energy variation times the actual distance a, i.e. $j_i' = am_i(u_i'^2 - u_i^2)/2$, divided by a suitable time-interval Δt. In order to get rid of the microscopic fluctuations, it is necessary to consider a sufficiently long Δt, so as to include a large number of collisions. Since the number of collisions is proportional to the system size, it is only in long systems that fluctuations can be removed without spoiling the slow dynamics of the heat flux. Equilibrium simulations show that for $L/N = a/2$ the leading contribution to the heat flux is given by the term j_i' which exhibits a low-frequency divergence with an exponent $\delta = 0.45$, that is not only definitely larger than 1/3 (the value predicted for the KPZ class), but is also fairly close to the results found for the FPU-β model [65].

In out-of-equilibrium simulations, a compatible exponent $\alpha = 0.4$ has been measured [81]. Those values should be compared with $\alpha = 1/2$, the prediction of mode-coupling theory, thus supporting the conjecture that the case $P = 0$ belongs to a universality class different from KPZ.

To conclude this section, let us mention that further support to this scenario comes from a stochastic model of a chain of harmonic oscillators, subject to momentum and energy-conserving noise [4]. Indeed, one can prove that the dynamical exponents are different from the KPZ class, e.g. $\delta = 1/2$ [4] and $\alpha = 1/2$ [67]. Details about this class of models can be found in Chap. 5. The qualitative explanation is that, as the stochastic collisions occur independently of the actual positions, the effective interaction among particles is symmetric and thus equivalent to the $P = 0$ case. Notably, this remains true even if the harmonic potential is replaced by an anharmonic one, like the FPU-$\alpha\beta$ [5]. Finally, the application of kinetic theories to the β-FPU model [70, 78, 80] yields a non-KPZ behavior, $\alpha = 2/5$. We refer the reader to Chap. 4 for a detailed account.

1.4.4 Comparison with Simulations and Experiments

The theoretical predictions have been intensively investigated in the recent literature. A direct validation by numerical simulations is, to some extent, challenging and has been debated through the years [22]. Generally speaking, the available numerical estimates of α and δ may range between 0.25 and 0.44 [64]. As a matter of fact, even in the most favorable cases of computationally efficient models as the HPG, finite-size corrections to scaling are sizeable. In this case, α-values as diverse as 0.33 [40] and 0.25 [10] for comparable parameter choices have been reported. On the other hand, a numerically convincing confirmation of the $\alpha = 1/3$ prediction comes from the diffusion of perturbations [15]. We refer to Chap. 6 for some detailed numerics.

The ultimate goal would be of course the validation of the universality hypothesis in more realistic systems, possibly characterized by more than one degree of

freedom per lattice site. The first remarkable attempt was the application to the vibrational dynamics of individual single-walled carbon nanotubes, which can be in many respect considered as one-dimensional objects. Signature of anomalous thermal transport was first reported in molecular dynamics simulations in [72]. Note that this type of simulations involve complicated three-body interactions among carbon atoms, thus supporting the claim that toy models like ours can indeed capture some general features. We refer the reader to Chap. 7 for a critical discussion of molecular dynamics results on carbon-based material. Chapter 8 will report some experimental data on nanotubes and nanowires and discuss the current state of the art.

1.5 The Coupled Rotors Model

As discussed in the previous sections, one-dimensional anharmonic chains generically display anomalous transport properties. A prominent exception is the coupled rotors chain described by the equation of motion

$$\dot{q}_n = p_n\,, \quad \dot{p}_n = \sin(q_{n+1} - q_n) - \sin(q_n - q_{n-1})\,. \tag{1.43}$$

The model is sometime referred to as the Hamiltonian version of the XY spin chain. The energy flux is $j_n^e = \langle p_n \sin(q_{n+1} - q_n)\rangle$. As the interaction depends only on the angle differences, angular momentum is conserved and one may expect anomalous transport to occur. Nevertheless, molecular dynamics simulations have convincingly demonstrated normal diffusion [36, 38, 92].

There are two complementary views to account for this difference. In the general perspective of nonlinear fluctuating hydrodynamics, the chain "length" L defined as $L = \sum_n (q_{n+1} - q_n)$ is not even well defined, because of the phase slips of $\pm 2\pi$, so the corresponding evolution equation breaks down and normal transport is eventually expected. From a dynamical point of view, one can invoke that normal transport sets in due to the spontaneous formation of local excitations, the so-called *rotobreathers*, that behave like scattering centers [33]. Phase slips (jumps over the energy barrier), on their side, may effectively act as localized random kicks, that contribute to scatter the low-frequency modes, thus leading to a finite conductivity. In order to test the validity of this conjecture, one can study the temperature dependence of κ for low temperatures T, when jumps across barriers become increasingly rare. Numerics indicates that the thermal conductivity behaves as $\kappa \approx \exp(\eta/T)$ with $\eta \approx 1.2$. The same kind of dependence on T (although with $\eta \approx 2$) is found for the average escape time τ across the potential barrier: this can be explained by assuming that the phase slips are the results of activation processes.

An important extension is the 2D case, i.e. rotors coupled to their neighbors on a square lattice, akin to the celebrated XY-model. As it is well known, the latter is characterized by the presence of the so called Kosterlitz-Thouless-Berezinskii phase transition at a temperature T_{KTB}, between a disordered high-temperature phase and a

low-temperature one, where vortices condensate. It is likely that transport properties are qualitatively different in the two phases. Numerical simulations [18] performed on a finite lattice indeed show that they are drastically different in the high-temperature and in the low-temperature phases. In particular, thermal conductivity is finite in the former case, while in the latter it does not converge up to lattice sizes of order 10^4. In the region where vorticity is negligible ($T < 0.5$) the available data suggest a logarithmic divergence with the system size, analogous to the one observed for coupled oscillators (see next section). Close to T_{KTB}, where a sizable density of bounded vortex pairs are thermally excited, numerical data still suggests a divergence, but the precise law has not be reliably estimated.

1.6 Two-Dimensional Lattices

Heat conduction in $2D$ models of anharmonic oscillators coupled through momentum-conserving interactions is expected to exhibit different properties from those of $1D$ systems. In fact, extension of the arguments discussed in the previous sections predicts a logarithmic divergence of κ with the system size N at variance with the power-law predicted for the $1D$ case. Consideration of this case is not only for completeness of the theoretical framework, but is also of great interest for almost-2D materials, like graphene, that will be treated in the Chaps. 7 and 9.

Although the theory in this case if far less developed, there are several numerical evidences in favor of such logarithmic divergence. In [68], a square lattice of oscillators interacting through the FPU-β (see Eq. (1.11), with $k_3 = 0$) or the Lennard-Jones [see Eq. (1.13)] potentials, was investigated by means of both equilibrium and nonequilibrium simulations. The models are formulated in terms of two-dimensional vector displacements u_{ij} and velocities and $\dot{u}_{ij}$, defined on a square lattice containing $N_x \times N_y$ atoms of equal masses m and nearest-neighbor interactions. Periodic and fixed boundary conditions have been adopted in the direction perpendicular (y) and parallel (x) to the thermal gradient, respectively. Simulations for different lattice sizes have been performed by keeping the ratio N_y/N_x constant and not too small to observe genuine $2D$ features (in [68] $N_y/N_x = 1/2$ was chosen).

The simulations reveal several hallmarks of anomalous behavior: temperature profiles display deviations from the linear shape predicted by Fourier law and the size dependence of the thermal conductivity is well-fitted by a logarithmic law

$$\kappa = A + B \log N_x \,, \tag{1.44}$$

with A and B being two unknown constants. A consistent indication comes from the evaluation of the Green-Kubo integrand in the microcanonical ensemble. Indeed, the energy-current autocorrelation is compatible with a decay $1/t$ at large times.

Despite these first indications, the numerics turns out to be very difficult, which is not surprising in view of the very weak form of the anomaly, peculiar of the 2D case.

As a matter of fact very robust finite-size effects are observed in the calculations for other lattices, which well exemplify the difficulties in observing the true asymptotic behavior with affordable computational resources [90].

Another interesting issue concerns dimensional crossover, namely how the divergence law of the thermal conductivity will change from the 2D class to 1D class as N_y/N_x decreases. This issue has been studied for the two-dimensional FPU lattice in [93]. We refer to Chap. 6 for a further detailed discussion.

1.7 Integrable Nonlinear Systems

The harmonic crystal behaves as an ideal conductor, because its dynamics can be decomposed into the superposition of independent "channels". This peculiarity can be generalized to the broader context of integrable nonlinear systems. They are mostly one-dimensional models characterized by the presence of "mathematical solitons", whose stability is determined by the interplay of dispersion and nonlinearity. This interplay is expressed by the existence of a macroscopic number of *conservation laws*, constraining the dynamical evolution. Intuitively, the existence of freely travelling solitons is expected to yield ballistic transport, i.e. an infinite conductivity. From the point of view of the Green-Kubo formula, this ideal conducting behavior is reflected by the existence of a nonzero flux autocorrelation at arbitrarily large times. This, in turn, implies that the finite-size conductivity *diverges linearly with the system size*.

Although integrable models are, in principle, exactly solvable, the actual computation of dynamic correlations is technically involved. A more straightforward approach is nevertheless available to evaluate the asymptotic value of the current autocorrelation. This is accomplished by means of an inequality due to Mazur [73] that, for a generic observable $\mathscr{A}$, (with $\langle \mathscr{A} \rangle = 0$, where $\langle \ldots \rangle$ denotes the equilibrium thermodynamic average) reads

$$\lim_{\tau \to \infty} \frac{1}{\tau} \int_0^\tau \langle \mathscr{A}(t) \mathscr{A}(0) \rangle \, dt \;\geq\; \sum_n \frac{\langle \mathscr{A} \mathscr{Q}_n \rangle^2}{\langle \mathscr{Q}_n^2 \rangle} \quad , \tag{1.45}$$

where $\mathscr{Q}_n$ denote a set of conserved and mutually orthogonal quantities, ($\langle \mathscr{Q}_n \mathscr{Q}_m \rangle = \langle \mathscr{Q}_n^2 \rangle \delta_{n,m}$).

In the present context the most relevant example is the equal-masses Toda chain with periodic boundary conditions, defined, in reduced units, by the Hamiltonian

$$H \;=\; \sum_{n=1}^{N} \left[\frac{p_n^2}{2} + \exp(-r_n) \right] , \tag{1.46}$$

where $r_n = q_{n+1} - q_n$ is the relative position of neighboring particles. The model is completely integrable, since it admits N independent constants of the motion

[34, 43]. Lower bounds on the long time value of $\langle J(t)J(0)\rangle$ can be calculated through the inequality (1.45) [99]. The resulting lower bound to the conductivity is found to increase monotonously with the temperature. At low T, the growth is linear with a slope comparable to the density of solitons $N_s/N = (\ln 2/\pi^2)T$. This trend is interpreted as an evidence for the increasing contribution of thermally excited nonlinear modes to ballistic transport.

To conclude, let us also mention that Mazur-type of inequalities have been recently used as a theoretical basis for the study of thermoelectric coefficients. This is discussed in Chap. 10 of the present volume.

1.8 Coupled Transport

Up to this point we have restricted the discussion to models where just one quantity, the energy, is exchanged with external reservoirs and transported across the system. In general, however, the dynamics can be characterized by more than one conserved quantity. In such cases, it is natural to expect the emergence of coupled transport phenomena, in the sense of ordinary linear irreversible thermodynamics. Works on this problem are relatively scarce [6, 39, 54, 75]. Interest in this field has been revived by recent works on thermoelectric phenomena [12, 13, 84] in the hope of identifying dynamical mechanisms that could enhance the efficiency of thermoelectric energy conversion. This will be treated in detail in Chap. 10.

Here, we briefly discuss two models: a chain of coupled rotors and the discrete nonlinear Schrödinger equation, where the second conserved quantity is the momentum and the norm (number of particles), respectively.

1.8.1 Coupled Rotors

The evolution equation defined in (1.43) must be augmented to include the exchange of momentum with the external reservoirs,

$$\begin{aligned}\dot{p}_n = {} & \sin(q_{n+1}-q_n) - \sin(q_n - q_{n-1}) \\ & +\delta_{1n}\left(\gamma(F_+ - p_1) + \sqrt{2\gamma T_+}\,\eta_+\right) + \delta_{1N}\left(\gamma(F_- - p_N) + \sqrt{2\gamma T_-}\,\eta_-\right)\end{aligned} \tag{1.47}$$

where $F_\pm$ and $T_\pm$ denote the torque applied to the chain boundary and the corresponding temperature, respectively; γ is the coupling strength with the external baths and $\eta_\pm$ is a Gaussian white noise with unit variance. The effect of external forces on the Hamiltonian XY model has been preliminary addressed in [31, 46, 49].

As discussed in Sect. 1.5, (angular) momentum is conserved and one can, in fact, define the corresponding flux as $j_n^p = \sin(q_{n+1} - q_n)$. A chain of rotors is perhaps the simplest model where one can exert a gradient of forces that couples to heat

transport, giving rise to nontrivial phenomena, even though the transport itself is normal. For $F_+ = F_-$, all the oscillators rotate with the same frequency $\omega = F$, no matter which force is applied: no momentum flux is generated. In fact, what matters is the difference between the forces applied at the two extrema of the chain. Therefore, from now on we consider the case of zero-average force, i.e. $F_+ = -F_-$. In the presence of such a gradient of forces, the oscillators may rotate with different frequencies and, as a result, a coupling between angular momentum and energy transport may set in. In principle, one could discuss the same setup for general chains of kinetic oscillators, as (linear) momentum is conserved in that context too. However, nothing interesting is expected to arise. For a binding potential, like in the FPU model, the presence of an external force is akin to the introduction of a homogeneous, either positive or negative, pressure all along the chain. In fact, the pressure P is, by definition, equal to the equilibrium average of the momentum flux, $P = \langle j^p \rangle$ (at equilibrium, the r.h.s. is independent of n). On the other hand, if the potential is not binding [e.g., the Lennard-Jones chain (1.13)] and the applied force is equivalent to a negative pressure, the system would break apart.

In the presence of two fluxes, the linear response theory implies that they must satisfy the equations [84] (angular brackets denote an ensemble, or equivalently, a time average, assuming ergodicity)

$$\begin{aligned} \langle j^p \rangle &= -L_{pp} \frac{d(\beta\mu)}{dy} + L_{pe} \frac{d\beta}{dy} \\ \langle j^e \rangle &= -L_{ep} \frac{d(\beta\mu)}{dy} + L_{ee} \frac{d\beta}{dy} \,, \end{aligned} \tag{1.48}$$

where $y = n/N$, β is the inverse temperature $1/T$ (in units of the Boltzmann constant) and μ is the chemical potential, which, in the case of the coupled rotors, coincides with the average angular frequency $\omega_n = \langle p_n \rangle$. Finally, $\mathbf{L}$ is the symmetric, positive definite, 2×2 Onsager matrix. If $L_{ep} = 0$, the two transport processes are uncoupled.

In the case of the rotor chain, it is important to realize that a correct definition of the kinetic temperature requires subtracting the coherent contribution due to the nonzero angular velocity, i.e.

$$T_n = \langle (p_n - \omega_n)^2 \rangle \,.$$

The effect of coupling between energy and momentum transport is better understood by considering a setup where the two thermal baths operate at the same temperature T. Because of the flux of momentum, the temperature profile deviates from the value imposed at the boundaries. In Fig. 1.9 we show the results for $T = 0.5$ and $F = 1.5$ and two different system sizes. Notably, the temperature profile displays a peak in the central region [46], where it reaches a value around 1.2; the average frequency varies nonuniformly across the sample with a steep region in correspondence of the central hot spot. At the same time, the energy flux j^e is zero, so that the anomalous

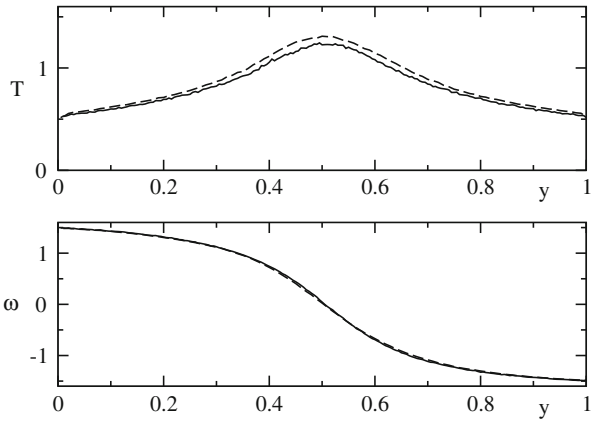

Fig. 1.9 Stationary profile of the temperature (*upper panel*) and of the average frequency (*lower panel*) for $T(0) = T(1) = 0.5$, $F = 1.5$, and $\gamma = 1$; $y = n/N$. The *dashed* and *solid curves* correspond to $N = 100$, and 200, respectively

behavior of the temperature profile is entirely due to the coupling with the nonzero momentum flux.

This behavior can be traced back to the existence of a (zero-temperature) boundary-induced transition. In fact, for $T = 0$, there exists a critical torsion $F_c = 1/\gamma$ [49] such that for $F < F_c$ the ground state is a twisted fully-synchronized state, whereby each element is at rest and is characterized by a constant phase gradient. Here, $T_n = 0$ throughout the whole lattice. For $F > F_c$ the fully synchronized state turns into a chaotic asynchronous dynamics with $\omega_1 = F = -\omega_N$. Remarkably, even though both heat baths operate at zero temperature and the equations are deterministic and dissipative, the temperature in the middle raises to a finite value (see Fig. 1.10) even in the thermodynamic limit.

The phenomenon can be interpreted as the onset of an interface (the hot region) separating two different phases: the oscillators rotating with a frequency F (on the left) from those rotating with a frequency $-F$ (on the right). The phenomenon is all the way more interesting in view of the anomalous scaling of the interface width with the system size (it grows as $N^{1/2}$, see Fig. 1.10) and its robustness (it is independent of the value of the torsion F, provided it is larger than the critical value F_c [49]).

Accordingly, the interface is neither characterized by a finite width nor it is extensive. A more careful inspection reveals that the $N^{1/2}$ width is due to a spatial Brownian-like behavior of an instantaneously much thinner interface. Nevertheless, even the instantaneous interface extends over a diverging number of sites, of order $N^{1/5}$, thus leaving the anomaly fully in place. Such a state can neither be predicted within a linear-response type of theory, nor traced back to some underlying equilibrium transition. Even more remarkably, it constitutes an example of a highly inhomogeneous, unusual chaotic regime. Indeed, while the fractal dimension is

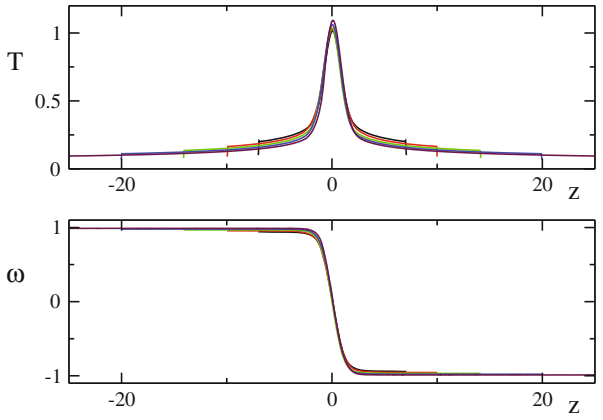

Fig. 1.10 Stationary profile of the temperature (*upper panel*) and of the average frequency (*lower panel*) for $T(0) = T(1) = 0.$, $F = 1.05$, and $\gamma = 1$; $z = (n - N/2)/N^{1/2}$. The various curves correspond to $N = 200$, 400, 800, 1600, and 3200

extensive (i.e. proportional to the number of oscillators) the Kolmogorov-Sinai (KS) entropy is not: it increases only as $N^{1/2}$. The KS entropy measures the diversity of the "ground state" non-equilibrium configurations that are compatible with the given thermal baths. Its lower-than-linear increase with N implies that we are not in the presence of a macroscopic degeneracy, as in spin glasses.

The anomaly of the regime is finally reinforced by the scaling behavior of the momentum flux, which scales as $N^{-1/5}$. A theoretical explanation of this behavior is still missing. All of these anomalies disappear as soon as the temperature at the boundaries is selected to be strictly larger than zero. In particular, the width of the hot spot suddenly becomes extensive and the scaling of the momentum is normal ($j^p \simeq 1/N$). The nonmonotonous behavior of the temperature is nevertheless a nontrivial consequence of the coupling between heat and momentum transport.

1.8.2 The Discrete Nonlinear Schrödinger Equation

The above discussed non-equilibrium transition is not a peculiarity of the rotor model. A similar scenario can be observed also in the Discrete Nonlinear Schrödinger (DNLS) equation [30, 51], a model with important applications in many domains of physics. In one dimension, the DNLS Hamiltonian is

$$H = \frac{1}{4}\sum_{n=1}^{N}\left(p_n^2 + q_n^2\right)^2 + \sum_{n=1}^{N-1}\left(p_n p_{n+1} + q_n q_{n+1}\right) \quad , \tag{1.49}$$

where the sum runs over the N sites of the chain. The sign of the quartic term is positive, while the sign of the hopping term is irrelevant, due to the symmetry associated with the canonical (gauge) transformation $z_n \to z_n e^{i\pi n}$ (where $z_n \equiv (p_n + \imath q_n)/\sqrt{2}$ denotes the amplitude of the wave function). The equations of motion are

$$i\dot{z}_n = -z_{n+1} - z_{n-1} - 2|z_n|^2 z_n \tag{1.50}$$

with $n = 1, \cdots, N$, and fixed boundary conditions ($z_0 = z_{N+1} = 0$). The model has two conserved quantities, the energy and the total norm (or total number of particles)

$$A = \sum_{n=1}^{N} (p_n^2 + q_n^2) = \sum_{n=1}^{N} |z_n|^2 \quad , \tag{1.51}$$

so that it is a natural candidate for the study of coupled transport.

Since the Hamiltonian is not the sum of a kinetic and potential energy, the thermal baths cannot be described by standard Langevin equations. An effective strategy has been proposed in [48]. Here below we report the evolution equation for the first oscillator, in contact with a thermal bath at temperature T_+ and with a chemical potential μ_+ (a similar equation holds for the last particle at site N)

$$\begin{aligned} \dot{p}_1 &= -(p_1^2 + q_1^2)q_1 - q_2 - \gamma\left[(p_1^2 + q_1^2)p_1 + p_2 - \mu_+ p_1\right] + \sqrt{2\gamma T_+}\xi_1' \\ \dot{q}_1 &= (p_1^2 + q_1^2)p_1 + p_2 - \gamma\left[(p_1^2 + q_1^2)q_1 + q_2 - \mu_+ q_1\right] + \sqrt{2\gamma T_+}\xi_1'' \quad , \end{aligned} \tag{1.52}$$

where γ measures the coupling strength with the thermal bath, while ξ_1' and ξ_1'' define two independent white noises with unit variance. It can be easily seen that the deterministic components of the thermostat, are gradient terms. As a result, in the absence of thermal noise, they would drive the system towards a state characterized by a minimal $(H - \mu A)$. Notice the nonlinear structure of the dissipation terms in Eq. (1.52).

An additional problem of the DNLS model is the determination of the temperature, as one cannot rely on the usual kinetic definition (this is again a consequence of the nonseparable Hamiltonian). An operative definition can be, however, given by adopting the microcanonical approach [83], i.e. by invoking the thermodynamic relationships,

$$T^{-1} = \frac{\partial \mathscr{S}}{\partial H} \quad , \quad \frac{\mu}{T} = -\frac{\partial \mathscr{S}}{\partial A} \, ,$$

where $\mathscr{S}$ is the entropy. As shown in [35, 47], the partial derivative $\partial \mathscr{S}/\partial C_i$ ($i = 1, 2$, with $C_1 = H$ and $C_2 = A$) can be computed by exploiting the fact that C_i is a conserved quantity,

$$\frac{\partial \mathscr{S}}{\partial C_i} = \left\langle \frac{W\|\boldsymbol{\xi}\|}{\boldsymbol{\nabla} C_i \cdot \boldsymbol{\xi}} \, \boldsymbol{\nabla} \cdot \left(\frac{\boldsymbol{\xi}}{\|\boldsymbol{\xi}\| W} \right) \right\rangle \tag{1.53}$$

where $\langle\,\rangle$ stands for the microcanonical average,

$$\boldsymbol{\xi} = \frac{\nabla C_1}{\|\nabla C_1\|} - \frac{(\nabla C_1 \cdot \nabla C_2)\nabla C_2}{\|\nabla C_1\|\|\nabla C_2\|^2} \tag{1.54}$$

$$W^2 = \sum_{\substack{m,n=1 \\ m<n}}^{2N} \left[\frac{\partial C_1}{\partial x_m}\frac{\partial C_2}{\partial x_m} - \frac{\partial C_1}{\partial x_n}\frac{\partial C_2}{\partial x_m} \right]^2 ,$$

and $x_{2n} = q_n$, $x_{2n+1} = p_n$. The resulting definitions of T and μ have the unpleasant property of being nonlocal: numerical simulations, however, show that they give meaningful results even when they are implemented for relatively short subchains.

As for the fluxes, they are naturally defined from the continuity equations for energy and norm

$$j_n^e = \dot{q}_n q_{n-1} + \dot{p}_n q_{n-1} \qquad j_n^p = q_n p_{n-1} - p_n q_{n-1} \,, \tag{1.55}$$

Notice that for the sake of simplicity we still use the same notations as in the previous setup although here j_n^p denotes the flux of norm/mass rather than momentum.

If one sets $T_+ = T_- = 0$, as in the XY model, the control parameter, i.e. the driving force, is given by $\delta\mu = |\mu_- - \mu_+|/2$ [48]. When $\delta\mu$ is larger than a critical value (that here depends on A), a bumpy temperature profile spontaneously emerges. As shown in Fig. 1.11, the left-right symmetry of the profile found in the XY model is lost, but the width of the peak still scales as $N^{1/2}$. A second crucial difference is the scaling behavior of the norm-flux, which decreases as $N^{-2/5}$ instead of $N^{-1/5}$. This suggests that more than one universality class is presumably present: the symmetry of the profile might play a crucial role.

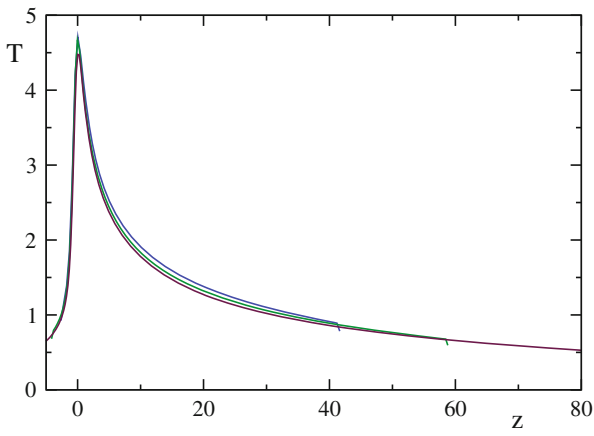

Fig. 1.11 Temperature profiles of the DNLS equation for 2000, 4000, 8000 and $T = 0$, $\mu_+ = 2$ and $\mu_- = 5$; $z = (n - \hat{n})/\sqrt{N}$, where $\hat{n}$ is the site with the highest temperature

In coupled transport, each conservation law implies the presence of a corresponding thermodynamic variable. In the case of the DNLS equation, there are two of them: the temperature T (or, equivalently β) and the chemical potential μ. If the extrema of a given system are "attached" to two different points in the (μ, T) space, a new question arises with respect to the transport of just one variable: the selection of the path in the phase plane. This problem can be solved with the help of the linear transport equations (1.48), which can be rewritten as

$$\frac{d\beta}{d\mu} = \frac{\langle j^e \rangle \beta L_{pp} - \langle j^p \rangle \beta L_{ep}}{\langle j^e \rangle \left(L_{pe} - \mu L_{pp}\right) - \langle j^p \rangle \left(L_{ee} - \mu L_{ep}\right)} \,. \tag{1.56}$$

The above first order differential equation can be solved once the Onsager matrix is known across the thermodynamics phase-diagram and the ratio of the two fluxes is given. This determines unambiguously the resulting temperature and chemical-potential profiles.

It is worth recalling that in the absence of a mutual coupling between the two transport processes (zero off-diagonal elements of the Onsager matrix) such curves would be vertical and horizontal lines in the latter representation. It is remarkable that the solid lines, which correspond to $j^e = 0$, are almost vertical for large μ: this means that in spite of a large temperature difference, the energy flux is very small. This is an indirect but strong evidence that the nondiagonal terms are far from negligible.

The condition of a vanishing particle flux $j^p = 0$ defines the Seebeck coefficient which is $S = -d\mu/dT$. Accordingly, the points in Fig. 1.12, where the dashed

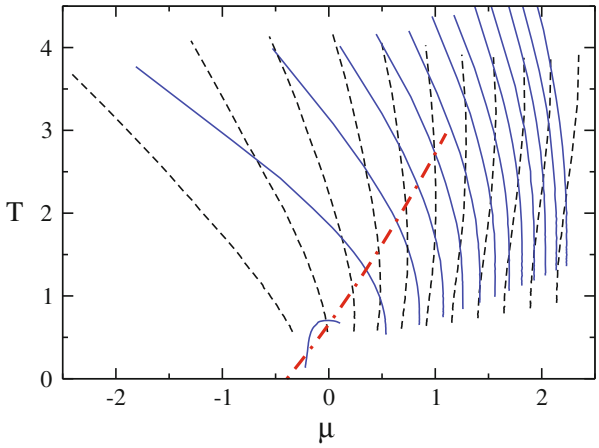

Fig. 1.12 Zero-flux curves in the (μ, T) planes. *Black dashed lines* correspond to $j^p = 0$ and are obtained with norm-conserving thermostats upon fixing the total norm density a_{tot}, T_L and T_R. *Blue solid lines* are for $j^e = 0$ using energy-conserving thermostats with fixed total energy density h_{tot}, μ_L/T_L and μ_R/T_R. Simulations are for a chain of length $N = 500$. The *thick dot-dashed lines* identify the locus where S changes sign (see text) (Color figure online)

curves are vertical identify the locus where S changes sign. The $j^e = 0$ curves have no direct interpretation in terms of standard transport coefficients.

1.9 Conclusions and Open Problems

In the previous sections we have seen that various theoretical approaches predict the existence of two universality classes for the divergence of heat conductivity in systems characterized by momentum conservation. Although this scenario is generally confirmed by numerical simulations, some exceptions have been found as well. The most notable counterexample is the normal conduction which emerges in chains of coupled rotors. As we have already discussed in Sect. 1.5, it is quite clear that the peculiarity of this model is to be traced back to the 2π-slips of the angles q_n.

Further, less-understood, anomalies have been found in models where q_n is a genuine displacement variable. One example is a momentum conserving modification of the famous "ding-a-ling" model. The system is composed of two kinds of alternating point particles (A and B): the A particles mutually interact via nearest-neighbour harmonic forces; the B particles are free to move and collide elastically with the A particles. Equilibrium and non-equilibrium numerical simulations indicate that the thermal conductivity κ is finite [59].

Normal heat transport in accordance to Fourier law has been claimed also in simulations of the FPU-$\alpha\beta$model (and of other asymmetric potentials), at low-enough energies/temperatures [97]. More detailed numerical simulations, however, indicate that the unexpected results for asymmetric potentials do not represent the asymptotic behavior [16, 91], but rather follow from an insufficient chain length. This if further strengthened in [56] where mode-coupling arguments have been used to determine the frequency below which finite-size effects are negligible. It turns out that, in some cases, the asymptotic behavior may only be seen at exceedingly low frequencies (and thereby exceedingly large system-sizes).

More recent studies report a finite thermal conductivity in the thermodynamic limit for potentials that allow for bond dissociation (like e.g Lennard-Jones, Morse, and Coulomb potentials) [37, 85]. This is explained by invoking phonon scattering on the locally strongly-stretched loose interatomic bonds at low temperature and by the many-particle scattering at high temperature. Nevertheless, the hard-point gas, a model where "dissociation" arises automatically, without the need to overcome an energy barrier, is found to exhibit a clean divergence of the conductivity. On the other hand, the universality of scaling in this model has been recently challenged by numerical studies of the hard-point gas with alternate masses and thermal baths at different temperatures acting at the boundaries. When the mass ratio is varied, the anomalous exponent is found to depart significantly from the value 1/3 predicted by the nonlinear fluctuating hydrodynamics [45].

Irrespective whether the above discrepancies are a manifestation of strong finite-size corrections, or of the existence of other universality classes, where the standard hydrodynamic theories do not apply, they have to be explained.

Acknowledgements We wish to thank L. Delfini and S. Iubini for their effective contribution to the achievement of several results summarized in this chapter.

References

1. Aoki, K., Kusnezov, D.: Bulk properties of anharmonic chains in strong thermal gradients: non-equilibrium ϕ^4 theory. Phys. Lett. A **265**(4), 250 (2000)
2. Aoki, K., Kusnezov, D.: Fermi-Pasta-Ulam β model: boundary jumps, Fourier's law, and scaling. Phys. Rev. Lett. **86**(18), 4029–4032 (2001)
3. Barabási, A.L., Stanley, H.E.: Fractal Concepts in Surface Growth. Cambridge University Press, Cambridge (1995)
4. Basile, G., Bernardin, C., Olla, S.: Momentum conserving model with anomalous thermal conductivity in low dimensional systems. Phys. Rev. Lett. **96**, 204303 (2006)
5. Basile, G., Delfini, L., Lepri, S., Livi, R., Olla, S., Politi, A.: Anomalous transport and relaxation in classical one-dimensional models. Eur. Phys. J.: Spec. Top. **151**, 85–93 (2007)
6. Basko, D.: Weak chaos in the disordered nonlinear Schrödinger chain: destruction of Anderson localization by Arnold diffusion. Ann. Phys. **326**(7), 1577–1655 (2011)
7. Blumen, A., Zumofen, G., Klafter, J.: Transport aspects in anomalous diffusion: Lévy walks. Phys. Rev. A **40**(7), 3964–3973 (1989)
8. Bonetto, F., Lebowitz, J.L., Rey-Bellet, L.: Fourier's law: a challenge to theorists. In: Fokas, A., Grigoryan, A., Kibble, T., Zegarlinsky, B. (eds.) Mathematical Physics 2000, p. 128. Imperial College, London (2000)
9. Casati, G.: Energy transport and the Fourier heat law in classical systems. Found. Phys. **16**(1), 51–61 (1986)
10. Casati, G., Prosen, T.: Anomalous heat conduction in a one-dimensional ideal gas. Phys. Rev. E **67**(1), 015203 (2003)
11. Casati, G., Ford, J., Vivaldi, F., Visscher, W.M.: One-dimensional classical many-body system having a normal thermal conductivity. Phys. Rev. Lett. **52**(21), 1861–1864 (1984)
12. Casati, G., Mejía-Monasterio, C., Prosen, T.: Increasing thermoelectric efficiency: a dynamical systems approach. Phys. Rev. Lett. **101**(1), 016601 (2008). doi:10.1103/PhysRevLett.101.016601
13. Casati, G., Wang, L., Prosen, T.: A one-dimensional hard-point gas and thermoelectric efficiency. J. Stat. Mech.: Theory Exp. **2009**(03), L03004 (2009)
14. Chang, C.W., Okawa, D., Garcia, H., Majumdar, A., Zettl, A.: Breakdown of Fourier's law in nanotube thermal conductors. Phys. Rev. Lett. **101**(7), 075903 (2008). doi:10.1103/PhysRevLett.101.075903
15. Cipriani, P., Denisov, S., Politi, A.: From anomalous energy diffusion to Lévy walks and heat conductivity in one-dimensional systems. Phys. Rev. Lett. **94**(24), 244301 (2005)
16. Das, S., Dhar, A., Narayan, O.: Heat conduction in the α-β Fermi-Pasta-Ulam chain. J. Stat. Phys. **154**(1–2), 204–213 (2014)
17. Das, S.G., Dhar, A., Saito, K., Mendl, C.B., Spohn, H.: Numerical test of hydrodynamic fluctuation theory in the Fermi-Pasta-Ulam chain. Phys. Rev. E **90**(1), 012124 (2014)
18. Delfini, L., Lepri, S., Livi, R.: A simulation study of energy transport in the Hamiltonian XY model. J. Stat. Mech.: Theory Exp. **2005**, P05006 (2005)
19. Delfini, L., Lepri, S., Livi, R., Politi, A.: Self-consistent mode-coupling approach to one-dimensional heat transport. Phys. Rev. E **73**(6), 060201(R) (2006)

20. Delfini, L., Denisov, S., Lepri, S., Livi, R., Mohanty, P.K., Politi, A.: Energy diffusion in hard-point systems. Eur. Phys. J.: Spec. Top. **146**, 21–35 (2007)
21. Delfini, L., Lepri, S., Livi, R., Politi, A.: Anomalous kinetics and transport from 1D self-consistent mode-coupling theory. J. Stat. Mech.: Theory Exp. **2007**, P02007 (2007)
22. Delfini, L., Lepri, S., Livi, R., Politi, A.: Comment on "equilibration and universal heat conduction in Fermi-Pasta-Ulam chains". Phys. Rev. Lett. **100**(19), 199401 (2008)
23. Delfini, L., Lepri, S., Livi, R., Politi, A.: Nonequilibrium invariant measure under heat flow. Phys. Rev. Lett. **101**(12), 120604 (2008)
24. Denisov, S., Klafter, J., Urbakh, M.: Dynamical heat channels. Phys. Rev. Lett. **91**(19), 194301 (2003)
25. Denisov, S., Zaburdaev, V., Hänggi, P.: Lévy walks with velocity fluctuations. Phys. Rev. E **85**(3), 031148 (2012)
26. Dhar, A.: Heat transport in low-dimensional systems. Adv. Phys. **57**, 457–537 (2008)
27. Dhar, A., Saito, K., Derrida, B.: Exact solution of a Lévy walk model for anomalous heat transport. Phys. Rev. E **87**, 010103 (2013)
28. Eckmann, J.P., Hairer, M.: Non-equilibrium statistical mechanics of strongly anharmonic chains of oscillators. Commun. Math. Phys. **212**(1), 105–164 (2000)
29. Eckmann, J.P., Pillet, C.A., Rey-Bellet, L.: Non-equilibrium statistical mechanics of anharmonic chains coupled to two heat baths at different temperatures. Commun. Math. Phys. **201**, 657 (1999)
30. Eilbeck, J.C., Lomdahl, P.S., Scott, A.C.: The discrete self-trapping equation. Physica D **16**, 318–338 (1985)
31. Eleftheriou, M., Lepri, S., Livi, R., Piazza, F.: Stretched-exponential relaxation in arrays of coupled rotators. Physica D **204**(3), 230–239 (2005)
32. Fermi, E., Pasta, J., Ulam, S.: Studies of nonlinear problems. Los Alamos Report LA-1940, p. 978 (1955)
33. Flach, S., Miroshnichenko, A., Fistul, M.: Wave scattering by discrete breathers. Chaos **13**(2), 596–609 (2003)
34. Flaschka, H.: The toda lattice. II. Existence of integrals. Phys. Rev. B **9**(4), 1924 (1974)
35. Franzosi, R.: Microcanonical entropy and dynamical measure of temperature for systems with two first integrals. J. Stat. Phys. **143**, 824–830 (2011)
36. Gendelman, O.V., Savin, A.V.: Normal heat conductivity of the one-dimensional lattice with periodic potential of nearest-neighbor interaction. Phys. Rev. Lett. **84**(11), 2381–2384 (2000)
37. Gendelman, O., Savin, A.: Normal heat conductivity in chains capable of dissociation. Europhys. Lett. **106**(3), 34004 (2014)
38. Giardiná, C., Livi, R., Politi, A., Vassalli, M.: Finite thermal conductivity in 1D lattices. Phys. Rev. Lett. **84**(10), 2144–2147 (2000)
39. Gillan, M., Holloway, R.: Transport in the Frenkel-Kontorova model 3: thermal-conductivity. J. Phys. C **18**(30), 5705–5720 (1985)
40. Grassberger, P., Nadler, W., Yang, L.: Heat conduction and entropy production in a one-dimensional hard-particle gas. Phys. Rev. Lett. **89**(18), 180601 (2002)
41. Hatano, T.: Heat conduction in the diatomic toda lattice revisited. Phys. Rev. E **59**, R1–R4 (1999)
42. Helfand, E.: Transport coefficients from dissipation in a canonical ensemble. Phys. Rev. **119**(1), 1–9 (1960). doi:10.1103/PhysRev.119.1
43. Hénon, M.: Integrals of the Toda lattice. Phys. Rev. B **9**(4), 1921 (1974)
44. Hu, B., Li, B., Zhao, H.: Heat conduction in one-dimensional chains. Phys. Rev. E **57**(3), 2992 (1998)
45. Hurtado, P.I., Garrido, P.L.: Violation of universality in anomalous Fourier's law (2015). arXiv preprint arXiv:1506.03234
46. Iacobucci, A., Legoll, F., Olla, S., Stoltz, G.: Negative thermal conductivity of chains of rotors with mechanical forcing. Phys. Rev. E **84**(6), 061108 (2011)
47. Iubini, S., Lepri, S., Politi, A.: Nonequilibrium discrete nonlinear Schrödinger equation. Phys. Rev. E **86**(1), 011108 (2012)

48. Iubini, S., Lepri, S., Livi, R., Politi, A.: Off-equilibrium Langevin dynamics of the discrete nonlinear Schrödinger chain. J. Stat. Mech.: Theory Exp. **2013**(08), P08017 (2013)
49. Iubini, S., Lepri, S., Livi, R., Politi, A.: Boundary-induced instabilities in coupled oscillators. Phys. Rev. Lett. **112**, 134101 (2014)
50. Kaburaki, H., Machida, M.: Thermal-conductivity in one-dimensional lattices of Fermi-Pasta-Ulam type. Phys. Lett. A **181**(1), 85–90 (1993)
51. Kevrekidis, P.G.: The Discrete Nonlinear Schrödinger Equation. Springer, Berlin (2009)
52. Klafter, J., Blumen, A., Shlesinger, M.F.: Stochastic pathway to anomalous diffusion. Phys. Rev. A **35**(7), 3081–3085 (1987). doi:10.1103/PhysRevA.35.3081
53. Kubo, R., Toda, M., Hashitsume, N.: Statistical Physics II. Springer Series in Solid State Sciences, vol. 31. Springer, Berlin (1991)
54. Larralde, H., Leyvraz, F., Mejía-Monasterio, C.: Transport properties of a modified Lorentz gas. J. Stat. Phys. **113**, 197–231 (2003)
55. Lee-Dadswell, G.: Universality classes for thermal transport in one-dimensional oscillator systems. Phys. Rev. E **91**(3), 032102 (2015)
56. Lee-Dadswell, G.R.: Predicting and identifying finite-size effects in current spectra of one-dimensional oscillator chains. Phys. Rev. E **91**, 012138 (2015)
57. Lee-Dadswell, G.R., Nickel, B.G., Gray, C.G.: Thermal conductivity and bulk viscosity in quartic oscillator chains. Phys. Rev. E **72**(3), 031202 (2005)
58. Lee-Dadswell, G.R., Nickel, B.G., Gray, C.G.: Detailed examination of transport coefficients in cubic-plus-quartic oscillator chains. J. Stat. Phys. **132**(1), 1–33 (2008)
59. Lee-Dadswell, G., Turner, E., Ettinger, J., Moy, M.: Momentum conserving one-dimensional system with a finite thermal conductivity. Phys. Rev. E **82**(6), 061118 (2010)
60. Lepri, S.: Relaxation of classical many-body Hamiltonians in one dimension. Phys. Rev. E **58**(6), 7165–7171 (1998)
61. Lepri, S., Politi, A.: Density profiles in open superdiffusive systems. Phys. Rev. E **83**(3), 030107 (2011)
62. Lepri, S., Livi, R., Politi, A.: Heat conduction in chains of nonlinear oscillators. Phys. Rev. Lett. **78**(10), 1896–1899 (1997)
63. Lepri, S., Livi, R., Politi, A.: On the anomalous thermal conductivity of one-dimensional lattices. Europhys. Lett. **43**(3), 271–276 (1998)
64. Lepri, S., Livi, R., Politi, A.: Thermal conduction in classical low-dimensional lattices. Phys. Rep. **377**, 1 (2003)
65. Lepri, S., Livi, R., Politi, A.: Universality of anomalous one-dimensional heat conductivity. Phys. Rev. E **68**(6, Pt 2), 067102 (2003). doi:10.1103/PhysRevE.68.067102
66. Lepri, S., Sandri, P., Politi, A.: The one-dimensional Lennard-Jones system: collective fluctuations and breakdown of hydrodynamics. Eur. Phys. J. B **47**(4), 549–555 (2005)
67. Lepri, S., Mejía-Monasterio, C., Politi, A.: Stochastic model of anomalous heat transport. J. Phys. A: Math. Theor. **42**, 025001 (2009)
68. Lippi, A., Livi, R.: Heat conduction in two-dimensional nonlinear lattices. J. Stat. Phys. **100**(5–6), 1147–1172 (2000)
69. Liu, S., Hänggi, P., Li, N., Ren, J., Li, B.: Anomalous heat diffusion. Phys. Rev. Lett. **112**(4), 040601 (2014)
70. Lukkarinen, J., Spohn, H.: Anomalous energy transport in the FPU-β chain. Commun. Pure Appl. Math. **61**(12), 1753–1786 (2008). doi:http://dx.doi.org/10.1002/cpa.20243
71. Mareschal, M., Amellal, A.: Thermal-conductivity in a one-dimensional Lennard-Jones chain by molecular-dynamics. Phys. Rev. A **37**(6), 2189–2196 (1988)
72. Maruyama, S.: A molecular dynamics simulation of heat conduction in finite length SWNTs. Physica B: Condens. Matter **323**(1), 193–195 (2002)
73. Mazur, P.: Non-ergodicity of phase functions in certain systems. Physica **43**(4), 533–545 (1969)
74. Meier, T., Menges, F., Nirmalraj, P., Hölscher, H., Riel, H., Gotsmann, B.: Length-dependent thermal transport along molecular chains. Phys. Rev. Lett. **113**(6), 060801 (2014)

75. Mejía-Monasterio, C., Larralde, H., Leyvraz, F.: Coupled normal heat and matter transport in a simple model system. Phys. Rev. Lett. **86**(24), 5417–5420 (2001)
76. Nakazawa, H.: On the lattice thermal conduction. Prog. Theor. Phys. Suppl. **45**, 231–262 (1970)
77. Narayan, O., Ramaswamy, S.: Anomalous heat conduction in one-dimensional momentum-conserving systems. Phys. Rev. Lett. **89**(20), 200601 (2002)
78. Nickel, B.: The solution to the 4-phonon Boltzmann equation for a 1D chain in a thermal gradient. J. Phys. A-Math. Gen. **40**(6), 1219–1238 (2007). doi:10.1088/1751-8113/40/6/003
79. Payton, D., Rich, M., Visscher, W.: Lattice thermal conductivity in disordered harmonic and anharmonic crystal models. Phys. Rev. **160**(3), 706 (1967)
80. Pereverzev, A.: Fermi-Pasta-Ulam β lattice: Peierls equation and anomalous heat conductivity. Phys. Rev. E **68**(5), 056124 (2003). doi:10.1103/PhysRevE.68.056124
81. Politi, A.: Heat conduction of the hard point chain at zero pressure. J. Stat. Mech.: Theory Exp. **2011**, P03028 (2011)
82. Pomeau, Y., Résibois, P.: Time dependent correlation functions and mode-mode coupling theories. Phys. Rep. **19**(2), 63–139 (1975)
83. Rugh, H.H.: Dynamical approach to temperature. Phys. Rev. Lett. **78**(5), 772 (1997)
84. Saito, K., Benenti, G., Casati, G.: A microscopic mechanism for increasing thermoelectric efficiency. Chem. Phys. **375**, 508–513 (2010)
85. Savin, A.V., Kosevich, Y.A.: Thermal conductivity of molecular chains with asymmetric potentials of pair interactions. Phys. Rev. E **89**(3), 032102 (2014)
86. Scheipers, J., Schirmacher, W.: Mode-coupling theory for the lattice dynamics of anharmonic crystals: self-consistent damping and the 1D Lennard-Jones chain. Z. für Phys. B Condens. Matter **103**(3), 547–553 (1997)
87. Schilling, R.: Theories of the structural glass transition. In: Collective Dynamics of Nonlinear and Disordered Systems, pp. 171–202. Springer, Berlin (2005)
88. Spohn, H.: Nonlinear fluctuating hydrodynamics for anharmonic chains. J. Stat. Phys. **154**(5), 1191–1227 (2014)
89. van Beijeren, H.: Exact results for anomalous transport in one-dimensional hamiltonian systems. Phys. Rev. Lett. **108**, 180601 (2012)
90. Wang, L., Hu, B., Li, B.: Logarithmic divergent thermal conductivity in two-dimensional nonlinear lattices. Phys. Rev. E **86**, 040101 (2012)
91. Wang, L., Hu, B., Li, B.: Validity of fourier's law in one-dimensional momentum-conserving lattices with asymmetric interparticle interactions. Phys. Rev. E **88**, 052112 (2013)
92. Yang, L., Hu, B.: Comment on "normal heat conductivity of the one-dimensional lattice with periodic potential of nearest-neighbor interaction". Phys. Rev. Lett. **94**, 219404 (2005)
93. Yang, L., Grassberger, P., Hu, B.: Dimensional crossover of heat conduction in low dimensions. Phys. Rev. E **74**(6), 062101 (2006)
94. Zaburdaev, V., Denisov, S., Hänggi, P.: Perturbation spreading in many-particle systems: a random walk approach. Phys. Rev. Lett. **106**(18), 180601 (2011)
95. Zaburdaev, V., Denisov, S., Klafter, J.: Lévy walks. Rev. Mod. Phys. **87**(2), 483 (2015)
96. Zhao, H.: Identifying diffusion processes in one-dimensional lattices in thermal equilibrium. Phys. Rev. Lett. **96**(14), 140602 (2006)
97. Zhong, Y., Zhang, Y., Wang, J., Zhao, H.: Normal heat conduction in one-dimensional momentum conserving lattices with asymmetric interactions. Phys. Rev. E **85**, 060102 (2012)
98. Zoia, A., Rosso, A., Kardar, M.: Fractional Laplacian in bounded domains. Phys. Rev. E **76**(2), 21116 (2007)
99. Zotos, X.: Ballistic transport in classical and quantum integrable systems. J. Low Temp. Phys. **126**(3–4), 1185–1194 (2002)